Economic Impact of Photovoltaic Power Forecast Error on Power System Operation in Japan

Yusuke Udagawa
The University of Tokyo
Tokyo, Japan
udagawa@iis.u-tokyo.ac.jp

Kazuhiko Ogimoto
The University of Tokyo
Tokyo, Japan
ogimoto@iis.u-tokyo.ac.jp

Joao Gari da Silva Fonseca Junior
The University of Tokyo
Tokyo, Japan
jfonseca@iis.u-tokyo.ac.jp

Hideaki Ohtake
The National Institute of Advanced Industrial Science and Technology
Tokyo, Japan
hideaki-ootake@aist.go.jp

Suguru Fukutome
JP Business Service Corporation
Tokyo, Japan
Suguru_Fukutome@jpbs.co.jp

Abstract—In this study, we analyzed the operational situation and cost for Tokyo Electric Power Company's service area by 2030, when a high penetration of variable renewable energy (VRE) sources will have been attained. Day-ahead unit commitment and real-time economic dispatch simulation were carried out by taking into account photovoltaic power yield forecasts and errors. The analysis allowed us to evaluate the economic impact of forecasting errors from VRE sources on the annual supply and demand balance within the target area. The analysis also showed that the use of day-ahead forecasting reduced the amount of unserved energy and shrank photovoltaic power yield curtailment in real-time operations.

Index Terms--Forecast Accuracy, Photovoltaic, Power Supply-Demand Balance, Unit Commitment

I. INTRODUCTION

The Strategic Energy Plan of Japan for the next decade was established in 2010 [1] and revised in 2014 [2]. According to the Plan in 2010, 53 GW of photovoltaic (PV) and 10 GW of wind power are expected to be installed by 2030. New feed-in tariff (FIT) programs were launched in Japan in July 2012. Owing to the high FIT prices for PV yield, the amount of installed and approved PVs reached 20.1 GW and 82.5 GW, respectively, in May 2015 [3]. The values are considerably higher than the plan's targets. Such levels of installed PV capacity are feared to make the operation of power systems more difficult. In this context, simulations of supply-demand for power in scenarios of high penetration of variable renewable energy (VRE) sources are of utmost importance, as they provide useful information to power systems operators and policy makers.

The objective of this study is to analyze the operational situation and projected costs for the Tokyo Electric Power Company service area in 2030. This area was chosen because it is the largest power balancing area in Japan and has high potential for PV deployment. The target year of the analysis and simulations is 2030, when high penetration of VRE sources is expected. The analysis was done using day-ahead (DA) unit commitment (UC) and real-time (RT) economic dispatch (ED) simulation.

In many power systems in Europe and the US, where VRE sources have already highly been installed, more installations are expected. DA UC is scheduled with electric demand and wind power and PV yield forecast based on weather predictions [4]. It is important to secure stable power system operations under the uncertainty of highly penetrated VRE sources. Recently, several studies that construct better large-scale PV yield forecasts have been conducted in Japan [5][6], and the actual PV yield data from Japanese power systems have also been compiled. Hence, the impact of PV yield forecast data and the error associated with actual PV yield data on future Japanese power system operations are evaluated in this study.

II. MODEL

Our UC model [7] must meet conventional constraints, mainly supply-demand balance and load frequency control (LFC) requirements, that is, secondary reserve. We adopted an interval UC approach. The model is formulated as a mixed-integer programming, and the objective function minimizes fuel and start-up costs for thermal generators not considering the cost for pumped storage generators. We refer to it as the operational cost in this study. The fuel cost is a function of the power output of thermal generators. Partial load efficiency is assumed to be followed by a piecewise linear curve. In addition, the model can consider confidence intervals (CI) of a VRE source forecast and ensure supply-demand balance and LFC reserve when the actual VRE power is within the CI. Further details about the model are available in the literature [7]. Some important constrains are as follows.

The aim of DA UC is to create schedules for each generator. We define $p_{n,t}$ as the electric power generated by

thermal generator *n* in time step *t*. We define $g_{m,t}$ and $h_{m,t}$ as the electric power generated and consumed by pumped storage generator *m* in time step *t*. In a VRE source, only the renewable electric power generated by PV is considered because the Tokyo area has a limited amount of wind resources. The forecasted amount of the electric power generated by PV in time step *t* is defined as $pv_t^{(f)}$. The scheduled generators can be dispatched to meet the forecasted demand $d_t^{(f)}$ at the lowest cost through the following constraints.

$$\sum_{n=1}^{N}(p_{n,t}) + \sum_{m=1}^{M}(g_{m,t} - h_{m,t}) + pv_t^{(f)} \geq d_t^{(f)} \ \forall_t \quad (1)$$

In (1), *N* is the number of thermal generators and *M* is number of pumped storage generators. The actual PV yield differed from the forecast PV yield because of the uncertainty of the forecast. To maintain the supply-demand balance in such a case, additional constraints using forecast error of PV yield are imposed:

$$\sum_{n=1}^{N}(\bar{p}_{n,t} - p_{n,t}) \geq pv_t^{(f)} - pv_t^{(fd)} \ \forall_t \quad (2)$$

$$pWk_{n,t} \cdot mxT_n \cdot (1 - blT_n) \leq \bar{p}_{n,t} \ \forall_{n,t} \quad (3)$$

$$\bar{p}_{n,t} \leq pWk_{n,t} \cdot mxT_n \ \forall_{n,t} \quad (4)$$

$$pWk_{n,t} \cdot (mnT_n + mxT_n) - \bar{p}_{n,t} \leq p_{n,t} \ \forall_{n,t} \quad (5)$$

$$p_{n,t} \leq \bar{p}_{n,t} \ \forall_{n,t} \quad (6)$$

$$\sum_{n=1}^{N}[p_{n,t} - pWk_{n,t} \cdot (mnT_n + mxT_n) + \bar{p}_{n,t}] \geq pv_t^{(fu)} - pv_t^{(f)} \ \forall_t \quad (7)$$

These equations model upward and downward reserves of functional thermal generators that can adjust their power outputs rapidly. The PV yield forecasts that include the upward and downward forecast errors are defined as $pv_t^{(fu)}$ and $pv_t^{(fd)}$, respectively. Here, $\bar{p}_{n,t}$ is the maximum power output of thermal generator *n* in time step *t*, excluding its LFC reserve. The variable $pWk_{n,t}$ represents a binary decision and it indicates whether thermal generator *n* in time step *t* works ($pWk_{n,t}$=1) or not ($pWk_{n,t}$=0). Variables mxT_n and mnT_n are the maximum and minimum electric power generated by thermal generator *n*.

The model also ensures an LFC reserve to handle system frequency deviations each time in step (8). The short-term variation due to electric load and PV yield variations is on the left-hand side in (8). We assumed that the load ($var_{d,t}$) and PV ($var_{pv,t}$) variations are in proportion to 3% of the demand forecast and 20% of the PV forecast $pv_t^{(fu)}$. Those values are typical when the analysis of Japanese power systems is conducted. The LFC reserve, supplied by thermal and pumped storage generators, is on the right-hand side in (8).

$$\sqrt{(var_{d,t})^2 + (var_{pv,t})^2} \leq \sum_{n=1}^{N}(pWk_{n,t} \cdot mxT_n - \bar{p}_{n,t}) \cdot 2 + \sum_{m=1}^{M}\begin{pmatrix} blP\_g_m \cdot mxP_m \cdot gWk_{m,t} \\ +blP\_h_m \cdot mxP_m \cdot hWk_{m,t} \end{pmatrix} \cdot 2 \ \forall_t \quad (8)$$

In (8), mxP_m represents the rated power generation of pumped storage generator *m*. Variables blT_n, blP_g_m, and blP_h_m show the contribution to the LFC capacity (Table I).

TABLE I. LOAD FREQUENCY CONTROL RESERVES

Parameter	Type		Pumping up	Generation
blT_n	Thermal power plants (Coal ,LNG, Oil)		—	5%
blP_g_m	Pumped storage power plants	Constant speed	—	16.5%
		Adjustable speed		
blP_h_m			10%	—

As there are many steep mountains in Japan, pumped storage hydro plants are common energy storages. Some important constraints regarding pumped storage generators are shown.

$$gWrk_{m,t} + hWrk_{m,t} \leq 1 \quad \forall_m, \forall_t \quad (9)$$

The variable $gWrk_{m,t}$ and $hWrk_{m,t}$ represent a binary decision of generating and pumping mode of pumped storage generator *m* in time step *t*, respectively. Each pumped storage generator cannot work as generating and pumping mode simultaneously. As there are many pumped storage generators in this study, some pumped storage generators can work as generating mode and the others can work pumping mode. The constraint for power output of pumped storage generator *m* in generating mode in time step *t* excluding its LFC reserve is as follows. mnP_m represents the minimum power generation of pumped storage generator *m*.

$$(mnP_m + blP\_g_m \cdot mxP_m) \cdot gWk_{m,t} \leq g_{m,t} \ \forall_m, \ \forall_t \quad (10)$$

$$g_{m,t} \leq (1 - blP\_g_m) \cdot mxP_m \cdot gWk_{m,t} \ \forall_m, \ \forall_t \quad (11)$$

As pumped storage generators (constant speed) cannot adjust inflow, power input in pumping mode is constant.

$$h_{m_c,t} = mxP_{m_c} \cdot hWk_{m_c,t} \ \forall_{m_c}, \forall_t \quad (12)$$

On the other hand, pumped storage generators (adjustable speed) can adjust power input in pumping mode. The constraints are excluded its LFC reserve.

$$(mnP_{m_a} + blP\_h_{m_a} \cdot mxP_{m_a}) \cdot hWk_{m_a,t} \leq h_{m_a,t} \ \forall_{m_a}, \forall_t \quad (13)$$

$$h_{m_a,t} \leq (1 - blP_{h_{m_a}}) \cdot mxP_{m_a} \cdot hWk_{m_a,t} \ \forall_{m_a}, \forall_t \quad (14)$$

The energy efficiency of each pumped storage generator was set to 70% (the energy loss rate due to pumping up and generating electricity is 30%). Each pumped storage generator was regarded as having a reservoir to simplify the model.

Regarding other constraints, that is, binary decisions concerning the start-up variable of thermal generators and the working variable of thermal and pumped storage generators, the upper and lower output limits of both generators, respectively, and the upper and lower storage limits of the pumped storage generators, details are shown in [7].

The constraints for RT ED are shown as follows. The power of each thermal generator is the only variable in RT ED. The constraint for supply-demand balance is set in (15). The actual amount of electric power generated by PV in time step t is denoted as $pv_t^{(a)}$. Those scheduled generators could be dispatched to meet actual demand $d_t^{(a)}$ at the lowest cost based on the generation schedules (On/Off) in DA UC. The operational schedules of pumping systems also follow the result of DA UC.

$$\sum_{n=1}^{N}(p_{n,t}) + \sum_{m=1}^{M}(g_{m,t} - h_{m,t}) + pv_t^{(a)} \geq d_t^{(a)} \ \forall_t \qquad (15)$$

III. DATA

Forecasts of solar irradiance (kW/m^2) were calculated using a mesoscale model (numerical weather prediction model) of the Japan Meteorological Agency (JMA) [8]. The regional solar irradiance data were calculated as the mean of the values observed in meteorological stations of JMA. To obtain the equivalent PV power generation (kW), the regional solar irradiance was multiplied by the system output coefficient (0.8). Both the PV power forecast and observations were calculated assuming a PV capacity of 17.5 GW in the Tokyo area. This value is calculated in proportion to the energy demand area based on the Japanese government's target in the Strategic Energy Plan in 2010, that is, a total of 53 GW in Japan by 2030. The solar irradiance observed and forecasted data were from FY 2010. The upper and lower CI were calculated using solar irradiance forecasting and observations from the previous year; CI was estimated for each time step and weather type (clearness index). Details are in [5][6]. The electric load data were assumed based on the electricity demand data in the Tokyo area in 2010 [9]. The electricity demand data, after the 2011 earthquake off the Pacific coast of Tohoku (2011.3.11), are affected by temporal action to save electricity. The demand data after the earthquake were revised to the standard level of electricity usage before the earthquake by using the relationship between temperature and electricity demand [10].

As this study focuses on the economic impact of PV yield forecasted on future power systems, prospects for future configuration of power plants are required. As part of the scenarios assumptions, we carried out a long-term power supply-demand analysis for power systems planning [11]. Those characteristics (capacity, efficiency, type of fuel, minimum operation, balancing capability, annual planned maintenance period, and failure rate), hourly load curves, and fuel prices were taken into account. Table II shows the values of n, m, t. Table III shows the supply capacity of thermal generators and pumped storage generators. In this study, the base load generators such as nuclear power plants and run-of-river hydro power plants are assumed to have a fixed output, that is, they are defined as must-run plants.

TABLE II. CONFIGURATION VALUES

Set	Value	Detail
T	48	Number of time step (Period of analysis: 24 hours)
N	92	Number of thermal power generators Coal: 15, LNG: 57, Oil: 20
M	52	Number of pumped storage power generators Pumped storage with adjustable speed: 11 (m_c) Pumped storage with constant speed: 41 (m_a)

TABLE III. SUPPLY CAPACITY OF POWER GENERATORS

	Type	Installed capacity	Detail
Peak & Middle load	Thermal	42.60 [GW]	Coal: 9.6 [GW] LNG: 22.16 [GW] Oil: 10.84 [GW]
	Pump	13.68 [GW]	Adjustable speed: 4.30 [GW] Constant speed: 9.38 [GW]
Base load	Nuclear	6.01 [GW]	—
	Hydro	5.14 [GW]	—
	Other	2.56 [GW]	—

TABLE IV. CASE (TYPES OF FORECASTS USED IN DA UC)

Case	Detail
Persistence	Persistence forecast, assuming the conditions at one time today will not change at the same time tomorrow.
Predict.	Day-ahead (DA) PV yield forecast without forecasting error
w/ 80% CI	DA PV yield forecast with forecasting error (80% CI)
w/ 90% CI	DA PV yield forecast with forecasting error (90% CI)
w/ 95% CI	DA PV yield forecast with forecasting error (95% CI)

IV. ANALYSIS

As our UC model can consider the forecast errors of PV yield, that is, CI, we calculated UC with five cases of PV yield forecast (Table IV). DA PV yield forecasts are based on the JMA's mesoscale model whose initial time of the forecast is 12:00 (JST) of the day preceding the target day. The forecast period is 33 hours ahead of time. UC and RT dispatch simulation periods are 24 hours (48 time steps) from 00:00 to 23:30. The forecast data are used starting from 00:00 in DA UC and RT dispatch.

At first, we calculated UC to meet the demand forecast including PV yield forecast with or without CI and obtained the schedules of the thermal generators (On/Off) and pumped storage generators (On/Off). In this study, we used actual

demand instead of forecasted demand in DA UC to simplify the analysis about the impact of VRE sources on power system operation. Using these schedules, we also dispatched the power of the thermal generators to meet the actual demand considering actual PV yield. In the cases considering PV yield forecast error, 80%, 90%, and 95% CIs were regarded as ranges where the forecast error could occur. The schematic image of the calculation flow is shown in Fig. 1.

Figure 1. Schematic flow of day-ahead unit commitment and real time dispatch simulation

V. RESULTS

The operational cost (fuel cost and start-up cost) as the expected value in DA UC are shown in Fig. 2. It is noted that the cost shown in this study does not include the cost of base load plants. The case where persistence forecast was used as forecast method had the lowest cost, followed in order by Predict, Predict. w/ 80% CI, w/ 90% CI, and w/ 95% CI. Fig. 2 shows that cost increases as CI increases. The upward and downward allowances (reserve) of thermal generators for the PV yield forecast error in DA UC increase as the CI increases. This behavior is associated with the modeling expressed by equations (2) and (7). A large CI also increases the number of operational (working) thermal generators under partial loading, which results in a cost increase. Fig. 3 shows the operational cost in RT ED. The results are similar to those in Fig. 2. Our UC model can assure the supply and demand balance in case that the PV yield forecast error in RT operation is within the CI in DA UC. PV yield forecast error outside the CI might occur in RT operation in time step *t*. In those cases, energy supply might fail to meet the demand. The cost in Fig. 3 does not include any penalty for an energy supply failure. Fig. 4 shows the amount of unserved energy which occurred during supply failures. In this case, the trend is completely changed compared with that in Fig. 3. The amount of unserved energy was the greatest in the case of a Persistence ratio of 1.07% of the total demand of 288 TWh in 2010. This result indicates the effect of the use of PV yield forecasting in DA UC. When a PV yield forecast is used to replace persistence (which is a very poor forecast), the amount of unserved energy is reduced considerably. Considering CI in DA UC reduces unserved energy even further: to 0.02% or 0.057 TWh a year in the case of Predict 95% CI. Fig. 5 shows the cost for unserved energy assuming JPY 25 (US 25 cents) per kWh, which represents a value equivalent to the average retail electricity cost in Japan. The value is sometimes referred as *value of lost load*, VOLL. Fig. 6 shows the total cost including the penalty cost (JPY 25/kWh) for unserved energy. The total cost is greatest in the case of Persistence. On the other hand, the absolute value of the difference between Persistence case and the other cases using PV yield forecast is larger. The lowest cost occurred in the case with 90% CI. In the cases of Persistence and Predict shown in Fig. 3, although the operating costs in RT ED are smaller than those in the cases where CI is used, the amount of unserved energy, that is, the penalty costs, are larger than that in the cases with a CI. Therefore, the total costs are larger. As the difference between the total costs in the cases using a CI is small, the order of the total costs depended mainly on the penalty cost.

VI. DISCUSSION

The duration curve of unserved energy in each case was calculated to estimate the required operating reserve for the PV yield forecasting error (not shown). Table V shows the amount of unserved energy (maximum and 99.5 percentile).

TABLE V. THE AMOUNT OF UNSERVED ENERGY

Case	Maximum	99.5 percentile
Persistence	4.8 GW	3.5 GW
Predict.	2.9 GW	1.3 GW
w/ 80% CI	2.8 GW	0.9 GW
w/ 90% CI	2.1 GW	0.6 GW
w/ 95% CI	1.4 GW	0.2 GW

Japanese power systems generally secure 8–10% of operating reserves based on forecasted maximum daily demand. The amount of average demand in the Tokyo service area in this study is around 39 GW. Even if 3.12 GW (8% of 39 GW) of operating reserve is secured by the power system, the maximum electric power shortage (unserved energy) without PV yield forecast, which is occurred in our simulations due to PV yield forecasting errors, cannot be avoided. The operating reserve, however, is secured for not only the PV yield forecasting error but also for various other faults in electrical power systems. On the one hand, more operating reserves will be needed in the near future if power systems are to maintain the supply-demand balance with highly installed VRE sources. On the other hand, considering the electric power shortage (at the 99.5 percentile), improvement of PV yield forecast technology can contribute to a reduction in the amount of required operating reserves. Securing operating reserves causes inefficiencies in thermal power plant

operations due to partial load operations and thus requires capital investment for combustion turbines in some cases. Therefore, forecasting technology has an even greater value than what is shown in this study.

Fig. 7 shows the required PV yield curtailment due to the shortage of LFC reserves. When the underestimation of PV yield forecast occurs over a considered CI, a shortage of LFC reserves follows. The result also indicates that PV yield forecasting technology mitigates the amount of curtailment. Recently, discussions regarding the necessity for curtailments have been thrust into the spotlight due to extensive installations of VRE sources [12]. Curtailment impacts both the security of power systems and the revenue of VRE projects. The discussion and demonstration of projects have begun in Japan. Achievement of optimal curtailment is the next problem to address.

VII. CONCLUSION

We have shown the economic impact generated by the uncertainty of PV yield forecasting on Japanese power system operations by 2030, when a high penetration of PV systems is expected. UC and ED simulations demonstrated that DA PV yield forecasts can strongly reduce the amount of unserved energy. Nevertheless, using a CI with DA PV yield forecasts does not significantly reduce it. Considering electric supply reliability, further reductions in unserved energy are needed. Even considering large PV yield forecast errors (at the 95% CI), hours with unserved energy still occur. On the one hand, our simulation also indicated that only using DA PV yield forecast in DA UC does not contribute to a reduction in the amount of PV yield curtailment. The amount is almost equivalent to the one obtained with a persistence forecast. On the other hand, using PV yield forecasts with a confidence interval in DA UC does reduce the amount of the curtailment.

Our result demonstrates that it is difficult to predict generation costs correctly because they depend on forecasting errors of VRE sources and the cost of unserved energy, that is, the cost of peak load plants or the cost of demand response. As the cost will be relevant to electricity market price, it will complicate to analyze the impact of the uncertainty and variability of VRE sources.

Our UC model can consider only DA PV yield forecast. There is no opportunity to revise the plant schedule. If re-scheduling (re-UC) could be accomplished a few hours before real time operation, unserved energy as shown above may be avoided. Recently, highly efficient energy generation technologies such as combined cycle gas turbines (CCGT) can start up in a few hours and modify the operational schedule when the PV yield forecast fails to meet the actual PV yield. In addition, relevant PV yield forecasting that is related to requirements for ancillary service, requires to improve our UC model and further analysis.

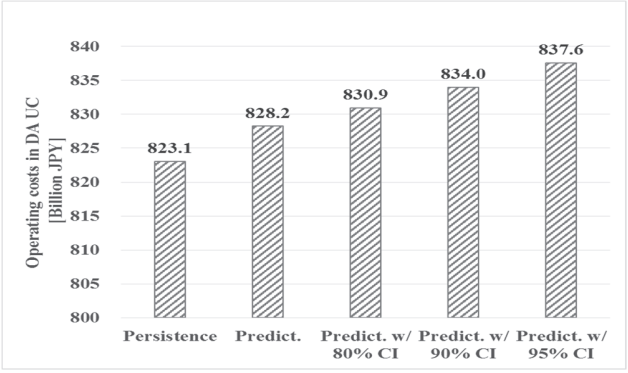

Figure 2. Operating costs in DA UC

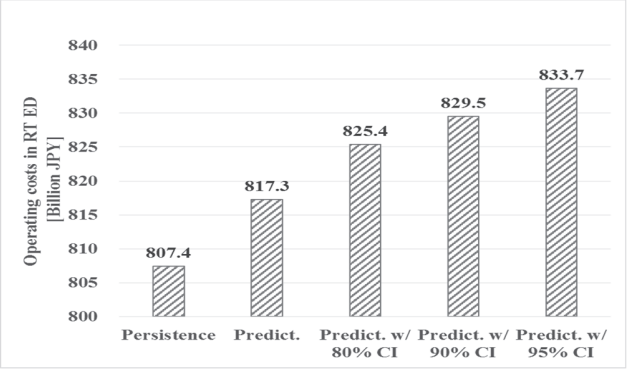

Figure 3. Operating costs in RT ED

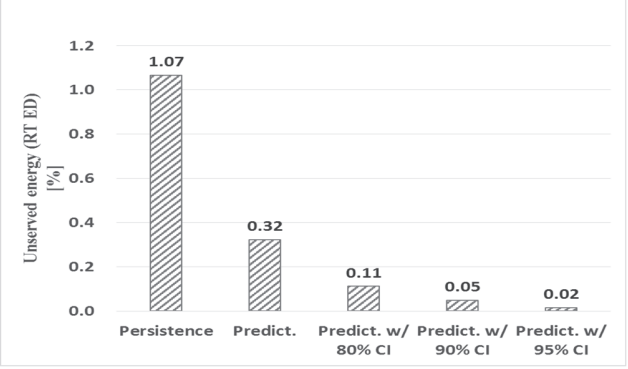

Figure 4. Unserved energy per total demand

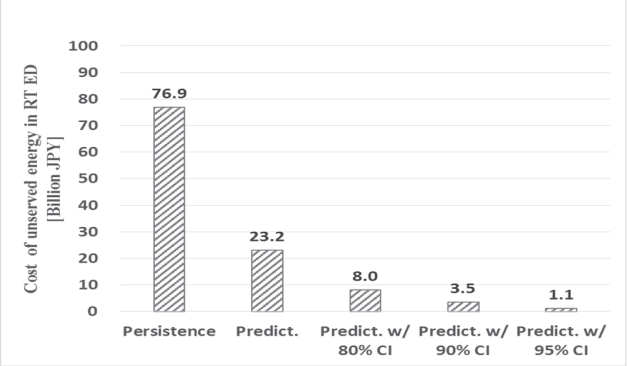

Figure 5. Cost of unserved energy in RT ED

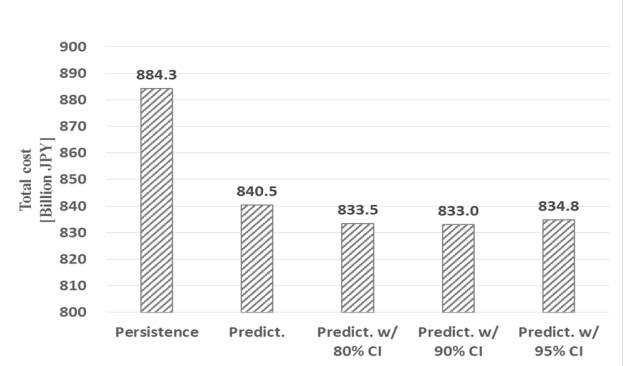

Figure 6. Total costs in RT ED

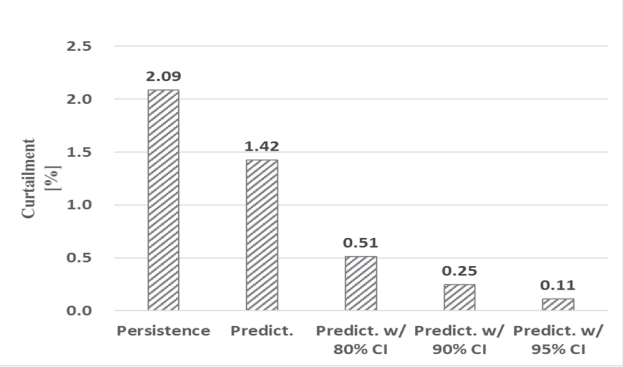

Figure 7. Required PV yield curtailment

REFERENCES

[1] Ministry of Economy, Trade and Industry, Agency for Natural Resources and Energy (2010, Jun.). Strategic Energy Plan [Online]. Available:http://www.enecho.meti.go.jp/category/others/basic_plan/pdf/100618honbun.pdf (in Japanese)

[2] Ministry of Economy, Trade and Industry, Agency for Natural Resources and Energy (2014, Apr.). Strategic Energy Plan [Online]. Available: http://www.enecho.meti.go.jp/en/category/others/basic_plan/pdf/4th_strategic_energy_plan.pdf

[3] Ministry of Economy, Trade and Industry, Agency for Natural Resources and Energy. Installed capacity of renewable energy [Online]. Available: http://www.enecho.meti.go.jp/category/saving_and_new/saiene/statistics/index.html (in Japanese)

[4] R. P. O'Neill, T. Dautel, and E. Krall., "Recent ISO software enhancements and future software and modeling plans," Federal Energy Regulatory Commission, Washington, D.C., Tech. Rep., 2011

[5] H. Ohtake, Joao Gari da Silva Fonseca Jr, T. Takashima., T. Oozeki, K-I. Shimose, and Y. Yamada, "Regional and seasonal characteristics of global horizontal irradiance forecasts obtained from the Japan Meteorological Agency mesoscale model", *Solar Energy, 116*, pp. 83-99. /doi:10.1016/j.solener., Mar 2015

[6] J. G. da S. Fonseca Junior, T. Oozeki, H. Ohtake, T. Takashima, and K. Ogimoto, "Regional forecasts of photovoltaic power generation according to different data availability scenarios: a study of four methods," *Prog. Photovolt. Res.* Appl., vol. 23, no. 10, pp. 1203–1218, Oct. 2015

[7] Y. Udagawa, K. Ogimoto, T. Oozeki, H. Ohtake, T. Ikegami, and S. Fukutome, "Development of Unit Commitment Model Considering Confidence Intervals of Photovoltaics Forecast and Analysis of a Large Scale Power System," *IEEJ Trans. EIS*, vol. 136, No.5, pp.484-496, 2016 (in Japanese)

[8] Japan Meteorological Agency (2013, Mar.). OUTLINE OF THE OPERATIONAL NUMERICAL WEATHER PREDICTION AT THE JAPAN METEOROLOGICAL AGENCY [Online]. Available: http://www.jma.go.jp/jma/jma-eng/jma-center/nwp/outline2013-nwp/index.htm

[9] Ministry of Economy, Trade and Industry: Electric power demand. [Online]. Available: http://www.meti.go.jp/setsuden/performance.html (in Japanese)

[10] S. Fukutome, H. Azuma, Y. Ikeda, Y. Iwafune, and K. Ogimoto, "A Power Demand Curve Estimation Method for a long-term power demand and supply analysis," in *Proc. 2011 IEE Japan Joint Technical Meeting on Frontier Technology and Engineering and Metabolism Society and Environmental Systems*, FTE-11-46, MES-11-32, pp.89-94, 2011 (in Japanese)

[11] K. Ogimoto, Y. Ikeda, K. Kataoka, T. Ikegami, and T. Oozeki, "Flexibility of Japan's Power System to Accommodate PV Penetration in 2030, " *EUPVSEC 27th European Photovoltaic Solar Energy Conference and Exhibition*, 6DO.12.6, 2012

[12] Bird, L., Cochran, J., and Wang, X, "Wind and solar energy curtailment: experience and practices in the United States, " US National Renewable Energy Laboratory, NREL/TP-6A20-60983, 3, 2014 [Online]. Available: http://www.nrel.gov/docs/fy14osti/60983.pdf